# 2

# An Overview of the Process of CT

In this chapter we describe, in the most general terms, the whole process of x-ray computerized tomography. Our intention is to give a brief overview. Hence, some terms with which the reader may not be familiar are introduced without proper definition. We ask the reader's indulgence; such terms will be carefully defined in subsequent chapters.

## 2.1 What Are We Trying to Do?

The aim of CT is to obtain information regarding the nature of material occupying exact positions inside the body. Generally speaking, the process as it is discussed in most of this book is as follows. A CT scanner is used to produce for a specified cross section of the body a sinogram, such as the one illustrated in Fig. 1.5(b). From this sinogram, we need to produce a two-dimensional image of the x-ray attenuation coefficient distribution in the cross section, as illustrated in Fig. 1.5(d).

In addition, the reconstruction of a series of parallel cross sections enables us to discover and display the precise shape of selected organs, as illustrated in Fig. 2.1. Such displays are obtained by further computer processing of the reconstructed cross sections (see Chapter 14).

## 2.2 Traditional Tomography

Prior to the introduction of CT, sectional imaging was done using various modes of (not computerized) *tomography*. We now describe a mode of tomography (*linear tomography*), illustrated in Fig. 2.2.

If we are interested in a cross section $C$ of a patient, we can obtain a fairly good estimate by the following tomographic method. We place a photographic plate $P$ parallel to the cross section $C$ on one side of the patient, and an x-ray source on the other side. By moving the x-ray source at a fixed speed parallel

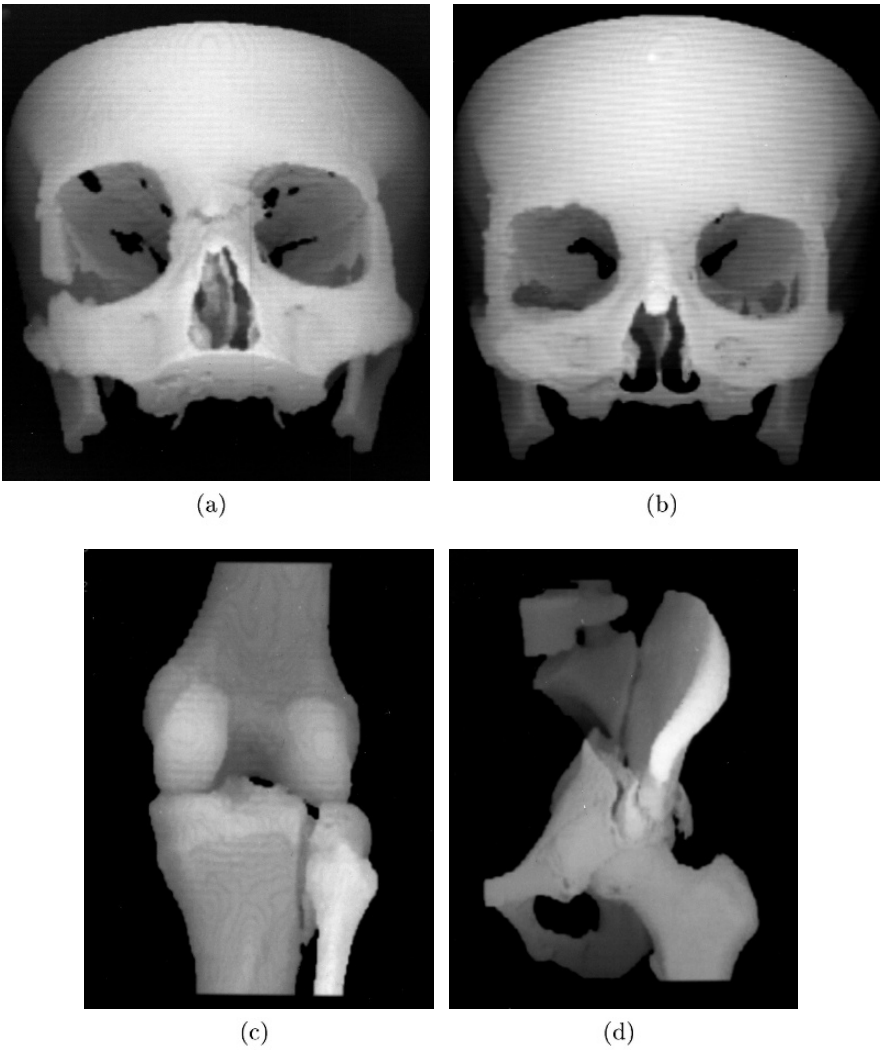


Fig. 2.1: Three-dimensional displays of bone structures of patients produced during 1986–8 by software developed in the author's research group at the University of Pennsylvania for the General Electric Company. (a) Facial bones of an accident victim prior to operation. (b) The same patient at the time of a one-year postoperative follow-up. (c) A tibial fracture. (d) A pelvic fracture.

to $C$ in one direction, and moving $P$ at an appropriate speed in the opposite direction, we can ensure that a point in $C$ always projects onto the same point in $P$, but a point in the patient above or below $C$ is projected onto different points in $P$. Thus on the photographic plate the section $C$ will stand out, while the rest of the body will be blurred out.

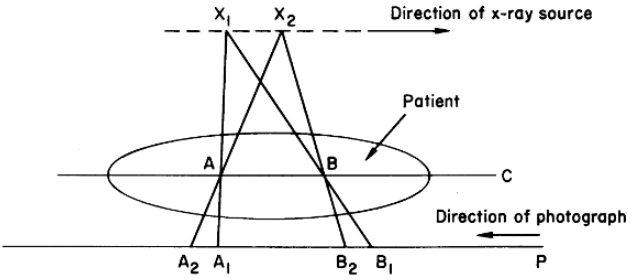


Fig. 2.2: Linear tomography. $C$: patient cross section; $A$ and $B$: two points in the cross section $C$; $X_1$ and $X_2$: positions of the x-ray source at times $t_1$ and $t_2$; $P$: the photographic plate; $A_1$ and $A_2$: positions of a fixed point on $P$ at times $t_1$ and $t_2$; $B_1$ and $B_2$: positions of another fixed point on $P$ at times $t_1$ and $t_2$. (Reproduced from [100], with permission from Elsevier.)

More closely related to CT is *transaxial tomography*. An example of this is shown in Fig. 2.3. The patient sits in a special rotating chair in an upright position. The x-ray film lies flat on a rotating horizontal table beside the patient. The table is positioned a little below the desired focal plane. X-rays are directed obliquely through the patient and onto the film. The x-ray tube remains stationary throughout the exposure. The patient and film both rotate in the same direction and at the same velocity. Only those points actually in the focal plane remain in sharp focus throughout a rotation. Points above and below the focal plane are blurred. The section thickness is determined by the angle between the x-ray tube and film. The more obliquely the central ray is directed toward the film the thinner is the tomographic section.

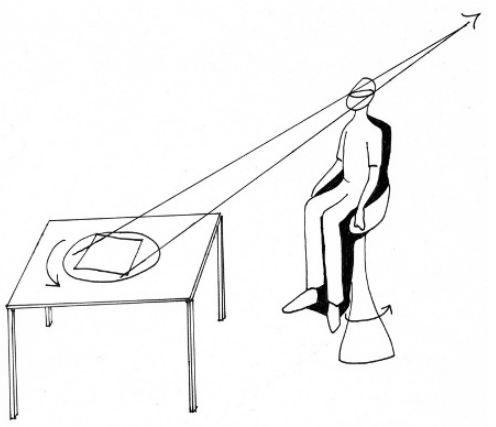

Fig. 2.3: Transaxial tomography.

In traditional forms of tomography, objects that are out of the focal plane are visible in the image, although in a blurred form. In CT, the images of cross sections are not influenced by the objects outside those sections. For this reason, the images produced by CT are much sharper, and hence generally of greater clinical utility. We will therefore forgo further discussion of traditional tomography and concentrate only on CT.

## 2.3 Data Collection for CT

A typical method by which data are collected for transverse section imaging in CT is indicated in Fig. 2.4. A large number of measurements are taken. Each of these measurements is related to an x-ray source position combined with an x-ray detector position. Both the source and the detector lie in the plane of the section to be imaged. For each combination of source and detector positions, two physical measurements are taken: a *calibration measurement* and an *actual measurement*. We now explain what these measurements are for a single fixed source and detector position combination.

During the calibration measurement, the object whose cross section we hope to image is not in the path of the x-ray beam from the source to the

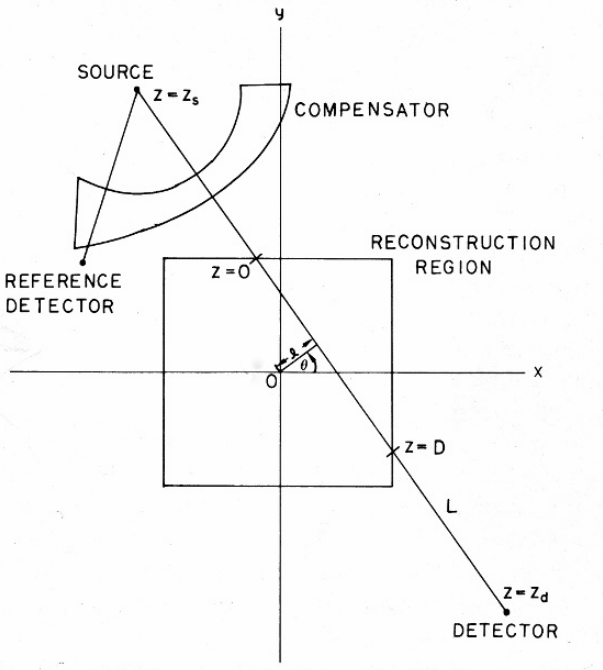


Fig. 2.4: Data collection for CT.

detector. In fact, it is assumed that the part of the beam that intersects the so-called *reconstruction region* (see Fig. 2.4) traverses through a homogeneous *reference material* such as air or water. The calibration measurement tells us how many out of a large but fixed number of photons that leave the source are counted by the detector. A *reference detector* serves the purpose of compensating for fluctuations in the strength of the x-ray source. Compensation can be done by dividing the number of photons counted by the detector by the number of photons counted by the reference detector. During the actual measurement, the object of interest is inserted into the reconstruction region, (partially) replacing the reference material. It is an important restriction that the object of interest does *not* occupy any point outside the reconstruction region. On the other hand, we allow the possibility of additional objects occupying fixed positions outside the reconstruction region during both the calibration and the actual measurement. An example of this is the object marked *compensator* in Fig. 2.4. (It compensates for the thinness of a transverse section of human body near the edges. This makes the number of photons reaching the detector at different positions more uniform and so reduces the range of photon counts that a detector needs to handle.) The actual measurement is defined in the same way as the calibration measurement, except that the cross section to be imaged is now in position. It influences the photon count by the detector, but not the photon count by the reference detector.

In summary, the size of the actual measurement as compared to the size of the calibration measurement depends on the photon absorbing and scattering properties of the object to be reconstructed as compared to those properties of a reference material.

We obtain a calibration measurement and an actual measurement for each of many source and detector position combinations. From these two sets of numbers we wish to produce a third set, namely, the set of CT numbers for the cross section of the object under investigation. These numbers, when coded into grayscale images, give the type of pictures that we see in Fig. 1.5(d). In the next section we discuss the physical interpretation of these numbers and images.

## 2.4 Voxels, Pixels, and CT Numbers

In a vacuum all x-ray photons that leave a source in the direction of a detector will reach the detector. When a material is placed between the source and the detector, some of the photons that leave the source in the direction of the detector will be removed from the beam (absorbed or scattered). The probability that a photon gets removed depends on the energy of the photon and on the material between the source and the detector.

The *linear attenuation coefficient* $\mu_{\bar{e}}^{t}$ of a tissue $t$ at energy $\bar{e}$ is defined as follows. Let $\rho$ be the probability that a photon of energy $\bar{e}$, which enters a uniform slab of the tissue $t$ of unit thickness, on a line $L$ perpendicular to

the face of the slab, will not be absorbed or scattered in the slab (i.e., $\rho$ is the transmittance at energy $\bar{e}$ of the slab along the line $L$, see Section 1.2 and especially Fig. 1.20). We define

$$\mu_{\bar{e}}^{t} = -\ln \rho, \tag{2.1}$$

where ln denotes the natural logarithm. Note that the size of the linear attenuation coefficient is dependent on the unit of length used. As is justified in Section 15.1, the linear attenuation coefficient is measured in units of inverse length. For example, the linear attenuation of water at 73 keV is 0.19 $\text{cm}^{-1}$.

In what follows we shall be working with the *relative linear attenuation* at energy $\bar{e}$. At any point of space, we define the relative linear attenuation to be $\mu_{\bar{e}}^{t} - \mu_{\bar{e}}^{a}$, where $t$ is the tissue occupying the point of space during the actual measurement and $a$ is the material occupying the point during the calibration measurement. Since we assume that the exterior of the reconstruction region is the same during the two sets of measurements, the relative linear attenuation is zero for all points outside the reconstruction region for all energies. Note also that for all points inside the reconstruction region $\mu_{\bar{e}}^{a}$ is the same, since the reference material is supposed to be homogeneous during the calibration measurement.

Now suppose that we are interested in a cross-sectional slice of the human body that is, say, 3 mm thick. We can subdivide this slice into small 3 mm long blocks with equal, square-shaped cross sections. These blocks are usually referred to as *volume elements*, or *voxels*, for short. Roughly speaking, a *CT number* is proportional to the average relative linear attenuation in a voxel. Since the relative linear attenuation itself is energy dependent, this definition needs further clarification, which is given in the next section. Typically, the background material is assumed to have the linear attenuation of water (thus the CT number of water is zero), and the scale of CT numbers is adjusted so that the CT number of air is approximately $-1000$.

Suppose, for example, that the reconstruction region in Fig. 2.4 is a square $41.6 \times 41.6$ $\text{cm}^2$, and we wish to use voxels that are $3 \times 0.65 \times 0.65$ $\text{mm}^3$. Then there is a $640 \times 640$ array of such voxels that exactly fills the reconstruction region, providing us with a $640 \times 640$ array of CT numbers. In displaying the cross section, we display the CT numbers. In this case, we want to display a $640 \times 640$ array of small squares, with the uniform grayness in each one being proportional to the CT number of the voxel in the appropriate position. These small squares are referred to as *picture elements*, or *pixels*, for short.

## 2.5 The Problem of Polychromaticity

When an x-ray beam passes through the body, its attenuation at any point depends on the material at that point and on the energy distribution (*spectrum*) of the beam. In CT the spectrum is made up from many energy levels

(*polychromatic*) and it changes (*hardens*) as the beam passes through the object. Thus, the attenuation at a point may vary with the direction of the beam passing through it. If we had a spectrum of only one energy level (*monochromatic*), this would not be the case. Each point would have a uniquely assigned attenuation coefficient, and reconstruction of the distribution of these coefficients would be a well-defined aim of computerized tomography.

We would like the following statement to be true: "The CT number assigned to a voxel is a property of the tissue occupying the voxel and does not depend on the location of the voxel in the slice." This is obviously desirable for diagnostic purposes. Also, as we shall see in the following, the truth of the statement is assumed in the development of mathematical procedures for calculating CT numbers.

A suitable definition for CT numbers is one in which a CT number is a multiple of the average relative linear attenuation of a voxel at a specified energy $\bar{e}$, to which we refer as the *effective energy.* Suppose now that we have a monochromatic x-ray source with photon energy $\bar{e}$. For a fixed position of the source and detector pair, let $C_m$ be the calibration measurement (the count of the number of photons that get from the source to the detector without the object to be reconstructed being between them, divided by the count of the reference detector), and let $A_m$ be the actual measurement (the count of the number of photons that get from the source to the detector with the object of interest in place, divided by the count of the reference detector). We define the *monochromatic ray sum*, $m$, for this beam by

$$m = -\ln\left(A_m/C_m\right), \tag{2.2}$$

and we refer to the set of $m$s for all source and detector pair positions as the *monochromatic projection data.* Based on the physical and mathematical facts to be discussed, we know that the relative linear attenuation inside the slice at the effective energy $\bar{e}$ can be accurately estimated from the monochromatic projection data.

In practice, the x-ray beam is polychromatic. Let $C_p$ and $A_p$ denote the calibration and actual measurement, respectively, for a particular source–detector pair position with the polychromatic x-ray beam. We define the *polychromatic ray sum, p,* for this x-ray beam by

$$p = -\ln\left(A_p/C_p\right), \tag{2.3}$$

and we refer to the set of $p$s for all source and detector pair positions as the *polychromatic projection data.*

Our problem is the following. For any source and detector position we can obtain $p$, but the reconstruction procedure requires $m$. The question naturally arises: Does $p$ uniquely determine $m$? Unfortunately, except in unrealistically restrictive cases, the answer is "no."

A more pragmatic question is: Given $p$, can we approximate $m$ well enough so that it leads to diagnostically useful CT numbers? There the answer appears to be "yes," as is illustrated in the following chapters.

## 2.6 Reconstruction Algorithms

We now briefly discuss the major topic of this book: the method for obtaining CT numbers from the monochromatic projection data. In practice, we apply this method using corrected polychromatic projection data in place of the (usually unavailable) monochromatic projection data.

Since we wish to implement our method on a computer, we need precise instructions on how the CT numbers are to be obtained from the monochromatic projection data. A finite sequence of unambiguous instructions that tell us how to get, step by step, from some given input to the desired output is an *algorithm*. Instructions that a physician writes up for unskilled laboratory assistants on what tests to perform next on a sample, based on the outcome of previous tests, should (and usually do) form an algorithm. The instructions provided by the Internal Revenue Service on how to fill out a tax return should also form an algorithm; the fact that they do not gives rise to the honorable profession of tax accountancy.

Basically the same procedure would have to be described differently depending on at whom the description is aimed. A computing machine needs a very detailed description (a computer program) in order to perform the same calculations that a mathematician would perform from just a few brief formulas.

In order to design an algorithm for obtaining CT numbers from monochromatic projection data, we first replace the problem by a simplified mathematical idealization of it. This has the same standing as the classical assumption one makes in calculating the earth's orbit; namely, that all the mass of the earth is concentrated in a single point at its center. While the assumption is blatantly false, as long as it leads to correct calculations, there is every reason to use it: it makes the theory and the resulting calculations tractable. There is very little we could do in calculating the earth's orbit if we had to know the location of every fly before such a calculation could be carried out.

The simplifying assumptions we make in setting up the theory for reconstruction algorithms are: (1) slices are infinitely thin; (2) for any particular source and detector pair position, all x-ray photons travel in the same straight line (which lies in the infinitely thin slice). A consequence of the first assumption is that the distinction between voxels and pixels disappears. Indeed, since the slice is infinitely thin, it can be thought of as a picture whose grayness at any point $(x, y)$ is proportional to the relative linear attenuation $\mu_{\bar{e}}(x, y)$ at that point. This is the reason why the theory behind reconstruction algorithms is often referred to as "image reconstruction from projections."

Let $L$ be the straight line that is the path of all the x-ray photons for a particular source–detector pair and let $m$ be the corresponding monochromatic ray sum. Based on our definition of a linear attenuation coefficient, it is proved in Section 15.2 that

$$m \simeq \int_0^D \mu_{\bar{e}}(x, y)\, dz. \tag{2.4}$$

In this formula, $\simeq$ denotes "approximately equal," $z$ is the distance of the point $(x, y)$ on the line $L$, and the integration limits 0 and $D$ are clear from Fig. 2.4.

Since $\mu_{\bar{e}}(x, y) = 0$ for points $(x, y)$ outside the reconstruction region, $\int_0^D \mu_{\bar{e}}(x, y)$ is the integral of $\mu_{\bar{e}}(x, y)$ along the line $L$. Thus our problem is to calculate the values of $\mu_{\bar{e}}(x, y)$ from estimates of its integrals along a number of lines, namely from the monochromatic projection data.

In some sense this problem was solved in 1917 by Radon. Let $\ell$ denote the distance of the line $L$ from the origin, let $\theta$ denote the angle made with the $x$ axis by the perpendicular drawn from the origin to $L$ (see Fig. 2.4), and let $m(\ell, \theta)$ denote the integral of $\mu_{\bar{e}}(x, y)$ along the line $L$. Radon proved (see Section 15.3) that

$$\mu_{\bar{e}}(x, y) = -\frac{1}{2\pi^2} \lim_{\varepsilon \to 0} \int_{\varepsilon}^{\infty} \frac{1}{q} \int_0^{2\pi} m_1(x \cos\theta + y \sin\theta + q, \theta)\, d\theta\, dq, \qquad (2.5)$$

where $m_1(\ell, \theta)$ denotes the partial derivative of $m(\ell, \theta)$ with respect to $\ell$. While the exact details of this formula are likely to be obscure to a non-mathematician, its implication should be clear: the distribution of the relative linear attenuations in an infinitely thin slice is uniquely determined by the set of *all* its line integrals.

This seems to indicate that the reconstruction problem has been solved since 1917. However, there are some practical difficulties in applying to CT this mathematical solution to the idealized problem:

(a) Radon's formula determines a picture from all its line integrals. In CT we have only a finite set of measurements. Even if these were *exactly* the projections along a number of straight lines, a finite number of them would not be enough to determine the picture uniquely, or even accurately. Based on the finiteness of the data alone one can easily produce objects for which the reconstructions will be very inaccurate (see Section 15.4).

(b) The measurements in computed tomography can only be used to estimate the line integrals. Inaccuracies in these estimates are due to the width of the x-ray beam, scatter, hardening of the beam, photon statistics, detector inaccuracies, etc. Radon's inversion formula is sensitive to these inaccuracies.

(c) Radon gave a mathematical formula; we need an *efficient* algorithm to evaluate it. This is not necessarily trivial to obtain. There has been a very great deal of activity to find algorithms that are fast when implemented on a computer and yet produce acceptable reconstructions in spite of the finite and inaccurate nature of the data. Much of this book is devoted to this topic.

## Notes and References

The mathematical and computational procedures underlying CT as described in this chapter are summarized in Fig. 2.5. Much of this material is based on [111]. A more up-to-date coverage of CT can be found in [155].

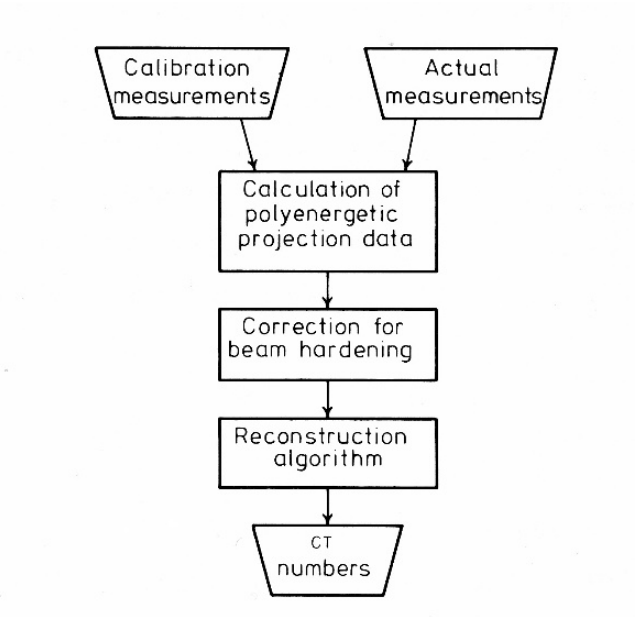


Fig. 2.5: Outline of the mathematical and computational procedures underlying CT. (Reproduced from [111]. Copyright by the Institute of Physics.)

The three-dimensional displays in Fig. 2.1 were produced by the software 3D98 [261], which was probably the first software system for 3D display and analysis that was integrated into a commercial CT scanner (namely the GE CT/T 9800).

The discussion of traditional tomography is based on [100]; see also [253]. These papers contain further early references. A more recent sample reference is [159] and a survey of relatively modern developments is given in [68].

The physics of x-ray generation and interaction with matter is discussed in books on radiological physics such as [54].

For a more detailed discussion on the nature of algorithms in general see, e.g., the relevant entries in [226]. A relatively recent book that discusses reconstruction-related algorithms is [211].

The Radon transform was introduced in [225]; that paper contains a derivation of the inversion formula (2.5).